Proceedings of the XIII International Conference "Ion Implantation and Other Applications of Ions and Electrons"

Effect of Carbon Ion Implantation and Xenon Ion Irradiation on the Tribological Properties of Titanium and Ti6Al4V Alloy

P. Budzyński[a,*], M. Kamiński[a], Z. Surowiec[b], M. Turek[b] and M. Wiertel[b]

[a] *Faculty of Mechanical Engineering, Lublin University of Technology, Nadbystrzycka 36, 20-618 Lublin, Poland*
[b] *Institute of Physics, M. Curie-Skłodowska University, Pl. Marii Curie-Skłodowskiej 1, 20-031 Lublin, Poland*

Doi: 10.12693/APhysPolA.142.713 *e-mail: p.budzynski@pollub.pl

Carbon implantation increases the coefficient of friction and wear for titanium, as well as eliminates oscillating changes in the coefficient of friction for titanium at a depth 25 times greater than the range of the implanted ions. Carbon implantation changes the characteristics of wear, namely the steel counter sample sticks to the surface layer of the titanium sample, and fragments of the sample are torn out during friction. Although the adhesive wear mechanism is dominant, abrasive and oxidative wear can also be observed. The application of additional xenon ion irradiation does not cause any significant changes in the wear characteristics. Implantation of the Ti6Al4V alloy with carbon ions reduces its coefficient of friction. This effect is opposite to that observed for technically pure titanium. Optimum tribological properties are obtained for the Ti6Al4V alloy, implanted with carbon ions with a fluence of 1×10^{17} C^+/cm^2. The different effects of carbon ion implantation and xenon ion irradiation on titanium and Ti6Al4V alloy result from differences between the energy distribution in the samples and the lack of chemical interactions of xenon atoms. The high energy deposited on the sample surface during the inelastic collision (S_e) with the target electrons induces significant changes in the surface topography of both metals. This also explains why the diamond-like carbon layer, which is formed as a result of carbon ion implantation, is removed after being irradiated with xenon ions.

topics: implantation, irradiation, synergy, coefficient of friction

1. Introduction

Titanium and its alloys are constructional materials used for devices operating in space, aviation and nuclear reactors, as well as for those operating in the high-ionizing radiation field. Owing to the good mechanical properties and corrosion resistance of titanium, it can be used in the design of new generation heavy ion accelerators [1, 2]; however, it has poor tribological properties. Various methods are used to improve tribological properties of materials. One method to improve the tribological properties of metals is the implantation of nitrogen ions [3–9] and carbon ions [10–12]. The implantation of carbon ion usually leads to a reduction of the coefficient of friction and wear of the materials. The interaction effects between the ions and the target depend on the energy of the ions. Ions with energies up to several hundred keV undergo energy loss, primarily due to elastic collision with the atomic nuclei of the target. The bombardment of the target by these ions is usually called implantation. Ions with energies above 1 MeV undergo energy loss, primarily as a result of inelastic collision with the electrons of the target. This interaction is traditionally known as irradiation. Primary point defects, which are produced during implantation and irradiation, migrate, undergo annealing (disappear) or form cascades of secondary defects. In multi-beam irradiation, the accumulation of radiation defects is described by the MSDA model [13, 14]. The study [15] has showed that partial annealing of defects by a higher energy beam was possible. In [16], oscillating changes were observed in crystal lattice parameters of titanium and Ti6Al4V alloy after irradiation with increasing fluence of swift xenon ions.

This study investigated the extent of changes in tribological properties of titanium and Ti6Al4V alloy induced by the 120 keV carbon ion implantation and the 160 MeV xenon ion irradiation. One of the objectives of this study was to determine if there is a synergistic effect of carbon ion implantation and xenon ion irradiation. Changes in mechanical properties after the implantation of carbon ions with energies up to several keV may result from radiation defects and chemical bonds formed

between the carbon atoms and the target components. Carbon implantation may cause the formation of diamond-like carbon (DLC) films, which are known for their excellent mechanical and tribological properties [17].

Changes induced by xenon ion irradiation can only result from changes in surface topography and radiation defects because xenon atoms are chemically inert and their concentration in the target is low due to low fluence compared to the concentration of implanted atoms.

The range of ions implanted in metals is small, usually below 1 μm. Changes in the tribological properties can be induced in the metal layer at a depth that is greater than the range of the implanted ions due to the long-range effect. The long-range effect was observed after the implantation of nitrogen ion in titanium and Ti6Al4V alloy [7] and several other metals [5, 6, 9, 18]. However, the long-range effect does not occur for every ion–target pair. For the cobalt alloy Stellite 6, the long-range effect occurs after implantation with nitrogen ions, but not with manganese ions [9].

The long-range effect has not yet been observed for the samples irradiated with swift xenon ions having energies of several hundred MeV [19]. Few studies to date have investigated changes in the tribological properties of irradiated metals [16, 20]. Irradiation with swift xenon and krypton ions produces new phases and changes the texture of the surface layer of titanium [21, 22], while irradiation with swift xenon ions increases its microhardness [22, 23].

Swift krypton ions cause also changes in the crystal structure of the Ti6Al4V alloy, leading to the formation of new phases [20]. On the other hand, irradiation with proton ions having an energy of 7 MeV with a fluence as high as 5×10^{17} p/cm^2 can lead to alloy element segregation [23]. The Ti6Al4V alloy irradiated with low fluences is characterised by increased microhardness [20], while the use of high fluences has practically no effect on its microhardness [23].

The main objective of this study was to observe changes in the tribological properties of titanium and its Ti6Al4V alloy implanted with nitrogen ions after the additional irradiation with swift xenon ions. The effect of irradiation on the friction process during the tribological test was investigated. We were also interested in whether the energy deposited in the electron system of samples during inelastic (S_e) collisions of xenon ions changes the surface topography of the material.

2. Experimental details

Specimens of technically pure titanium (Ti Grade 2) and Ti6Al4V alloy (Ti Grade 5) with a diameter of $\Phi = 25$ and a thickness of 3 mm were polished to obtain a surface roughness below 4 μm. Following surface treatment, the specimens

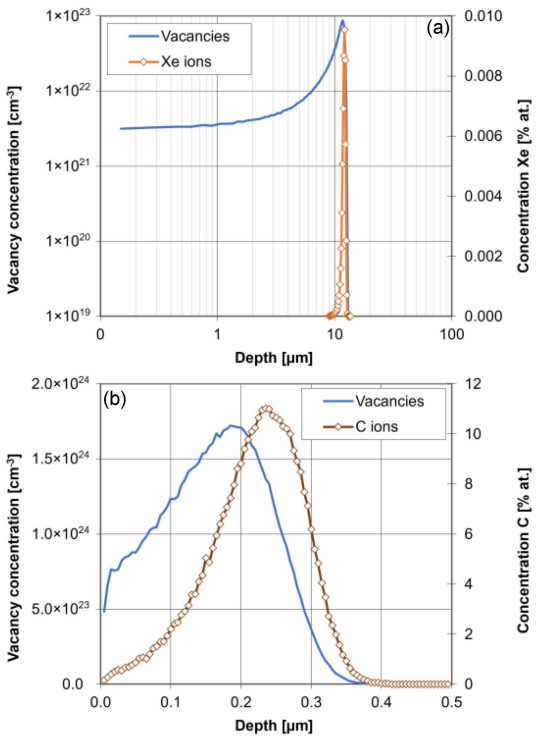

Fig. 1. Distribution of ions and defects along the titanium sample depth: (a) 160 MeV energy xenon ions irradiated with a fluence of 5×10^{14} Xe^{24+}/cm^2, (b) 120 keV energy carbon ions implanted with a fluence of 1×10^{17} C$^+$/cm^2.

were implanted with 120 keV carbon ions using a standard ion accelerator available at the Institute of Physics at Maria Curie-Skłodowska University in Lublin. Irradiation with 160 MeV xenon ions was performed on the IC-100 cyclotron (JINR Dubna). To ensure uniform irradiation, the ion beam was swept over the surface of the sample both vertically and horizontally.

The aluminium sample holder protruded outwards from the vacuum chamber and was air-cooled. The fluence of the ion beam did not exceed 2–8$\times10^{12}$ ions/m^{2}s, which limited the power introduced into the sample by the ion beam to 100–400 W/m^2. As a result, the temperature of the sample during irradiation did not exceed 60°C. The pressure in the chamber during irradiation was 1.1×10^{-9} Pa.

Microphotographs of the surface of the sample were taken with the AFM and Tescan Vega 3LMU scanning electron microscope (SEM) equipped with the X-ray microanalysis EDS and WDS systems. In the tribological tests, the coefficients of friction and wear were measured under technically dry friction conditions on a self-made pin/ball-on disc stand [24] and with the use of Nano Tribometer NTR^2 from Anton Paar (CFM Instrument). The counter sample was a 100Cr6 bearing steel ball with a diameter of $\Phi = 2$ mm, and the load was set to 300 mN. Wear was measured as the cross-sectional area of the wear

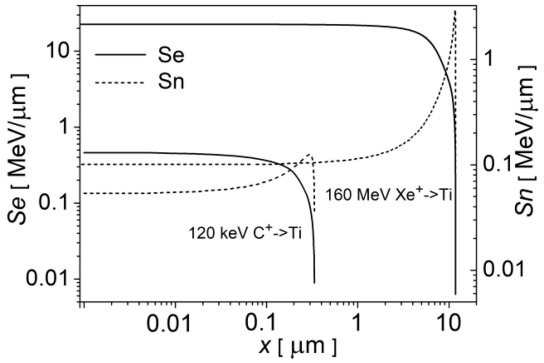

Fig. 2. Electron energy loss S_e and nuclear energy loss S_n of carbon and xenon ions for different penetration depths in titanium target.

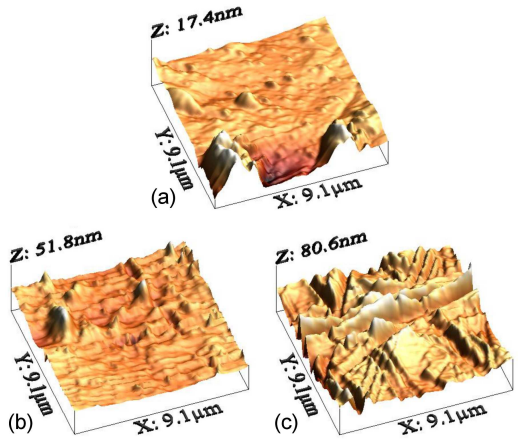

Fig. 3. AFM images of titanium samples: before implantation (a) and after implantation with carbon ions with a fluence of 5×10^{16} C^+/cm^2 (b), and after additional irradiation with xenon ions with a fluence of 5×10^{14} Xe^{24+}/cm^2 (c).

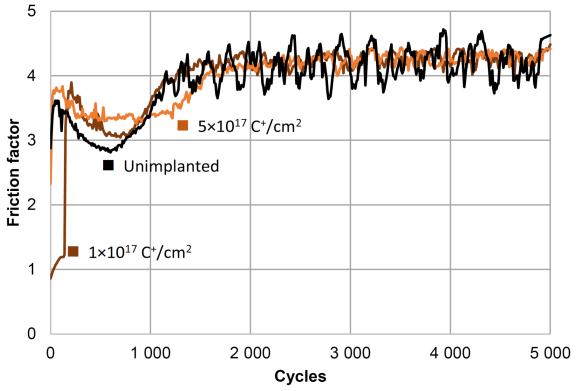

Fig. 4. Coefficient of friction for titanium implanted with carbon ions.

track made by the ball. Measurements of wear track were made with the Intra Form Talysurf profilometer and processed in Talymap Lite V7. Due to the irregular shape of the track, the wear was calculated based on 15 measurements (profilographs) made in different spots on the wear track circumference per every sample.

2.1. Implantation and irradiation of titanium

The stopping and range of ions in matter (SRIM) simulation [25] predicts the vacancies depth distribution, as well as C and Xe ion concentration depth profiles in titanium, shown in Fig. 1. Carbon ions are deposited on the surface layer with a thickness of 0.38 μm. Implantation-induced defects are located in the surface layer below the ion range (Fig. 1). Xenon ions are distributed in the layer toward the end of the range at depths in the range of 10–12.6 μm. Their number is considerably smaller, because the irradiation fluence was almost three times smaller. Defects are predominantly formed toward the end of the xenon ion range due to elastic collision with target atoms.

Energy losses caused by inelastic collisions of ions with target electrons (S_e) and elastic collisions with target atoms (S_n) are shown in Fig. 2.

Figure 3 shows the AFM images of the surface of the titanium samples before and after the implantation and irradiation. The polished surface of titanium shows the presence of small hills formed by oxides (Fig. 3a). After carbon implantation, the titanium surface unevenness increase due to the faster oxidation of the surface layer of the sample. The penetration of oxygen into the sample favors the radiation defects (Fig. 3b). These surface irregularities are visibly enhanced by additional irradiation with xenon ions (Fig. 3c). On the sample surface, one can see traces of local melting that occurred when the maximum fluence ion beam was swept over this surface. The melting of the sample surface is related to the local temperature increase in the site of the ion beam incidence. The temperature of the entire sample did not exceed 60°C.

Tribological tests were conducted on a pin-on-disc stand. Variations in the coefficient of friction (CoF) observed in the tests are shown in Fig. 4. At the beginning of the test, a thin layer with the face-centered cubic (fcc) structure is worn off, which was formed on the surface of the unimplanted sample during the mechanical sample preparation [21]. This layer is more ductile than that of the hexagon close-packed (hcp) structure materials [26], hence the CoF fluctuations are minor, and the CoF value first decreases and then increases. After this layer is worn off, the coefficient of friction shows large-amplitude oscillating fluctuations during the first 1200 tribological test cycles. In the range of about 1200–5000 test cycles, the coefficient of friction undergoes quasi-periodic fluctuations. The CoF results obtained for the carbon implanted samples (Fig. 4) should be analysed for the three areas: (i) on the surface of the sample where the DLC layer is formed; (ii) in the layer reached by the implanted carbon ions; and (iii) inside the inner layer of the

TABLE I

Wear of titanium and Ti6Al4V alloy after 5000 tribological test cycles.

Sample	Fluence $[C^+/cm^2]$	Fluence $[Xe^{24+}/cm^2]$	Wear $[\mu m^2]$
Ti	Unimplanted		2839(20)
Ti	5×10^{16}	0	6127(20)
Ti	5×10^{16}	5×10^{14}	3540 (20)
Ti	1×10^{17}	0	3227 (20)
Ti	1×10^{17}	5×10^{14}	2883 (20)
Ti6Al4V	Unimplanted		3748 (50)
Ti6Al4V	1×10^{16}	0	4858 (50)
Ti6Al4V	1×10^{16}	1×10^{14}	4031 (20)
Ti6Al4V	5×10^{16}	0	4302 (20)
Ti6Al4V	5×10^{16}	2.5×10^{14}	3538 (20)
Ti6Al4V	1×10^{17}	0	1260 (10)
Ti6Al4V	1×10^{17}	5×10^{14}	4202 (50)

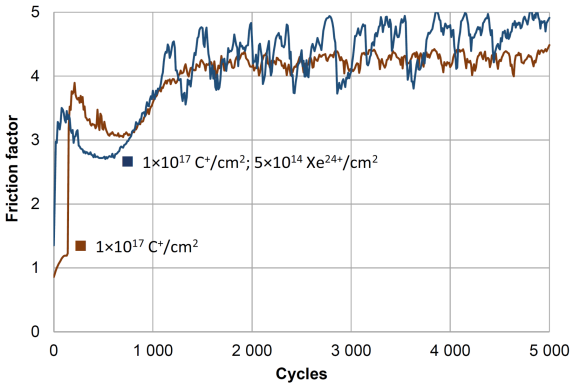

Fig. 5. Coefficient of friction for titanium implanted with carbon ions and irradiated with xenon ions.

sample. Carbon implantation leads to the formation of a thin DLC layer with a low coefficient of friction. The thickness of the layer increases with increasing ion fluence. The layer is clearly visible only after implantation with a fluence of 1×10^{17} C^+/cm^2. Nevertheless, this layer is not permanent and is worn off after about 200 tribological test cycles. When the layer is worn off, CoF of the carbon-implanted samples is higher than that of the unimplanted sample up to about 1200 tribological test cycles. Above 1500 tribological test cycles, the average coefficient of friction of the implanted samples is the same as that of unimplanted samples.

Carbon ion implantation slightly increases the value of the friction coefficient up to about 1000 tribological test cycles, but significantly decreases its fluctuations in the range of 1000–5000 cycles. This means that the decrease in fluctuations occurs at a depth greater than the initial range of the implanted carbon ions.

The use of high-energy irradiation with xenon ion after carbon implantation leads to a decrease in the value of the coefficient of friction at the beginning of the tribological test (up to 800 cycles) and significantly increases local changes (fluctuations) of CoF in the range of 1200–5000 cycles (Fig. 5), which is characteristic of the unimplanted sample.

Implantation of carbon ion changes the chemical composition of the surface layer and thus reduces the sticking effect between the steel ball and the target fragments. In the friction process, fragments of the unimplanted sample are displaced by the counter sample and deposited on the surface of the track, which is clearly seen in Fig. 6a. After implantation, the bottom of the track is smooth (Fig. 6b).

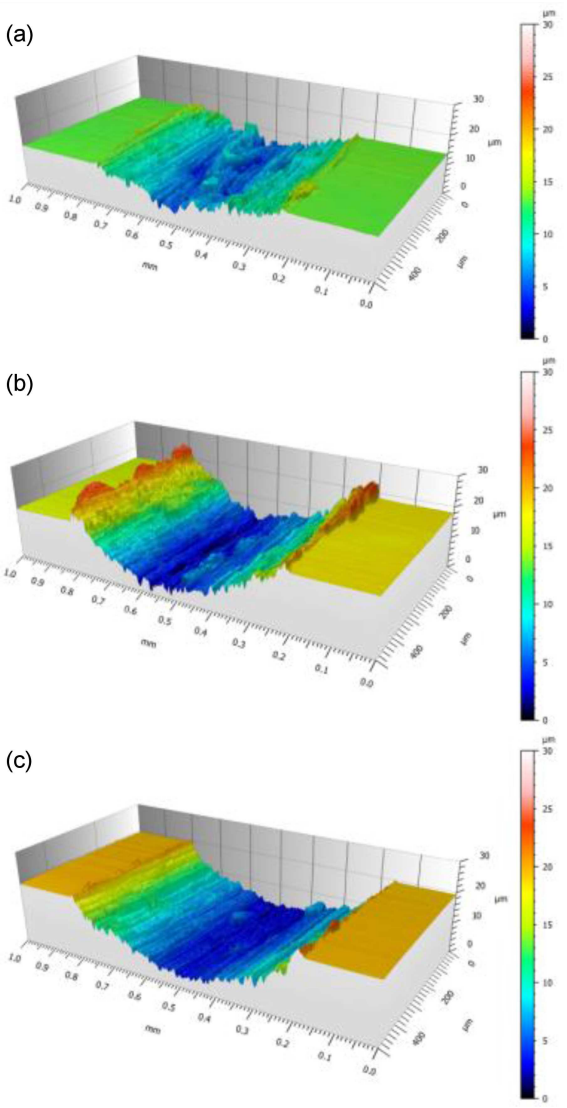

Fig. 6. 3D profilographs of the wear track for (a) Ti sample, (b) Ti sample after implantation with fluence 5×10^{16} C^+/cm^2, (c) Ti6Al4V alloy sample after implantation with fluence 1×10^{17} C^+/cm^2. All profilographs are made on the same scale.

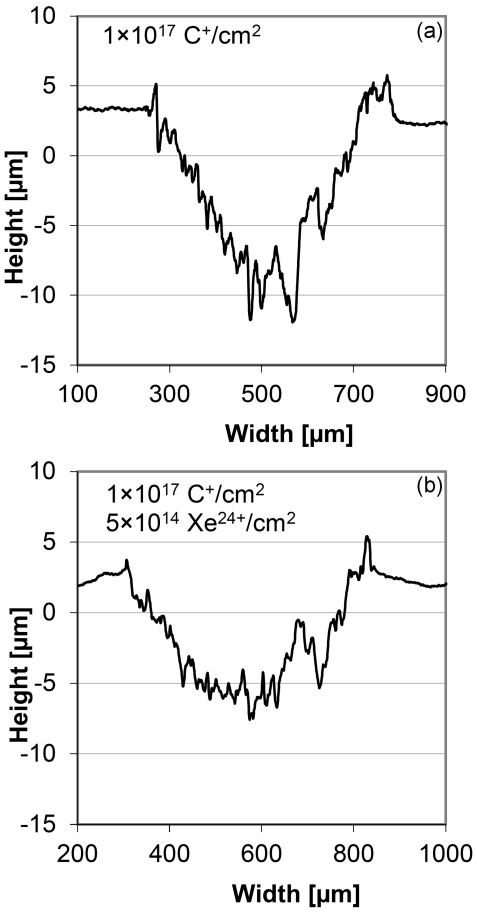

Fig. 7. Profilographs showing wear track on the titanium surface after 5000 tribological test cycles: (a) after implantation with carbon ions with fluence 1×10^{17} C^+ cm^{-2}, (b) after additional irradiation with xenon ions with fluence 5×10^{14} Xe^{24+}/cm^2.

Figure 7 shows typical profilographs of wear track on the titanium surface after 5000 tribological test cycles. After the carbon ion implantation, the track is deep and has numerous additional cavities on the walls (Fig. 7a). These cavities result from chipping and scratching induced by formed hard titanium carbides (TiC). After irradiation, a slight reduction in wear can be observed during the tribological test (see Fig. 7b).

The degree of wear in tribological tests was determined on the basis of the obtained wear track profilographs. Since the track has an irregular shape, the average value of the track cross-section measured in 20 spots along its entire length (on the track circumference) was taken as the measure of wear. Carbon implantation with fluence 5×10^{16} C^+/cm^2 increases the wear of titanium by 2.16 times, see Table I. After doubling the carbon ion fluence, the wear of this sample only increases by about 1.14 times compared to the unimplanted sample. Irradiation of pre-implanted titanium reduces its wear in tribological tests. The wear of a titanium sample pre-implanted with a fluence of 1×10^{17} C^+/cm^2 and subjected to additional xenon irradiation is similar to that of the unimplanted samples.

Figure 8 shows SEM photographs of wear tracks on the surface of the samples and the contents of carbon and oxygen along the marked scanning line of the elements playing a key role in the friction process. Carbon implantation causes an increase in wear (track width), see Fig. 8b. A change in the topography of the trace can be observed — on the smoothed surface of the track there are cavities formed by torn-out fragments of the sample. Carbon implantation changes wear characteristics. The presence of the implanted carbon causes sticking of the steel counter sample to the surface layer of titanium and tearing out fragments of the sample during friction. The mechanism of adhesive wear is dominant with the noticeable presence of abrasive and oxidative wear.

The carbon content on the surface of the sample is ~ 6 at.%. At the bottom of the track, at a depth ranging from 0 to 10 μm (the track's cross-section is V- or U-shaped, as shown in Fig. 7), the carbon content is constant and equal to ~ 1.7 at.% (Fig. 8b, c). Such carbon content is sufficient to eliminate the large CoF fluctuations that are characteristic of the unimplanted sample. It is worth noting that the carbon content in the track remains constant regardless of the depth of the track. This may indicate that some of the implanted carbon atoms formed hard TiC compounds that sculptured the surface of the track during friction, and then were removed from the friction node, as can be seen in the profilographs shown in Fig. 7. The remaining part of the implanted carbon diffuses deep into the sample and forms TiC at greater depths as the tribological test progresses. It should be noted that the implanted carbon ions have a range of only 0.42 μm, and their distribution in the implanted sample has a shape resembling an inverted letter V. This means the diffusion of carbon atoms deep into the friction zone with the simultaneous equalization of the concentration of carbon atoms throughout the friction zone. Hence, the final, post-tribological test distribution of carbon atom concentration is almost perfectly rectangular over the entire wear track area. The displacement of carbon atoms is made possible by radiation-accelerated diffusion, also due to the local increase in temperature during friction.

The diffusion of carbon atoms in the tribological test was first observed in [27]. Displacement of atoms and defects during the friction process, beyond the initial range resulting from the implantation process, can lead to a long-range effect [5–9, 18]. After carbon implantation, the CoF variations characteristic of the unimplanted sample disappear throughout tribological test until the track reaches a depth of 10 μm. This means that the effect of carbon implantation ranges to a depth that is 25 times greater than the initial range of the implanted carbon ions.

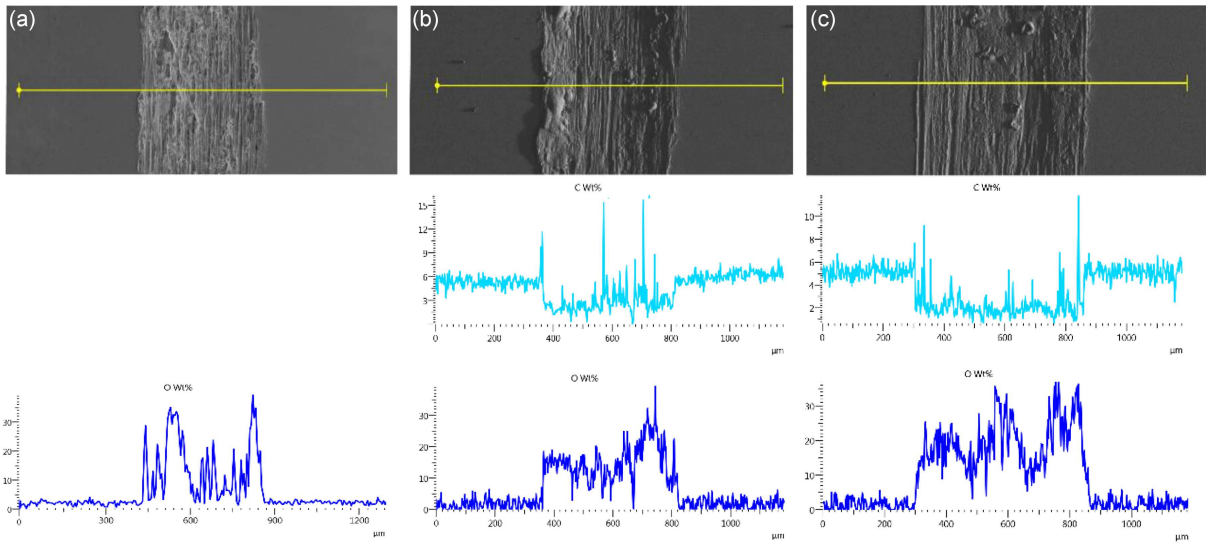

Fig. 8. SEM photographs of wear track on a Ti sample: (a) before implantation, (b) after implantation with carbon ions with fluence 5×10^{17} C^+/cm^2, (c) after additional irradiation with xenon ions with fluence 5×10^{14} Xe^{24+}/cm^2.

Following the additional irradiation with xenon ions (Figs. 6b, 7c and 8c), the characteristics of wear do not change significantly, despite the reduced sticking of the sample to fragments of the counter sample material, as evidenced by smaller cavities on the track surface (Fig. 8c). The average content of oxides in the sample implanted with fluence 1×10^{17} C^+/cm^2 is similar to that in the unimplanted sample and increases after xenon ion irradiation, see Fig. 8c. The degree of oxidative wear increases, which is facilitated by the penetration of oxygen deep into the sample along radiation defects and the formation of cavities on the sample surface during irradiation (Fig. 3c).

2.2. Implantation and irradiation of Ti6Al4V alloy

The polished surface of the Ti6Al4V alloy shows more irregularities (Fig. 9a) than that of pure titanium (Fig. 3a), due to the different abrasion resistance of the alloy components. Following the implantation (Fig. 9b), the surface of the Ti6Al4V alloy is also more irregular than that of technically pure titanium shown in Fig. 3b. This is due to the different sputtering ratios of the disc components. Surface irregularities increase after additional irradiation with high-energy xenon ions, see Fig. 9c.

The CoF results obtained for the Ti6Al4V alloy are presented in Fig. 10. The coefficient of friction shows small variations both before and after implantation, which has also been observed in other studies [28, 29]. In these studies, the variations were analysed by means of the Self-Organizing Neural Network algorithm. Carbon implantation reduces the coefficient of friction without changing the overall trend of CoF variations during the test. The decrease of CoF grows with the implanted ion fluence. Implantation with a fluence of 1×10^{17} C^+/cm^2

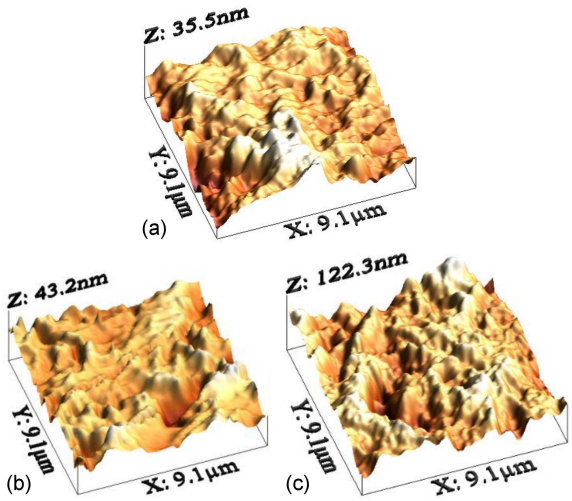

Fig. 9. AFM images of Ti6Al4V alloy: before implantation (a), after implantation with fluence 5×10^{16} C^+/cm^2 (b), after additional irradiation with high-energy xenon ions with a fluence of 1×10^{14} Xe^{24+}/cm^2 (c).

leads to the formation of a thin DLC layer, which is immediately worn off. The differences between the CoF values of implanted and unimplanted samples disappear above 2000 tribological test cycles.

Irradiation of pre-implanted Ti6Al4V alloy samples with high-energy xenon ions destroys the thin DLC layer and increases the CoF value by about 0.5, see Fig. 1. Above 1000 test cycles there are no CoF variations after additional irradiation with xenon ions, which is in fact a phenomenon observed for titanium samples that were prepared, implanted and irradiated in the same way (Fig. 5).

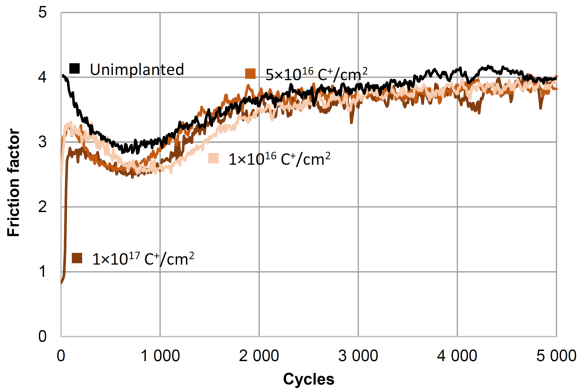

Fig. 10. Coefficient of friction for Ti6Al4V alloy before and after implantation with carbon ions.

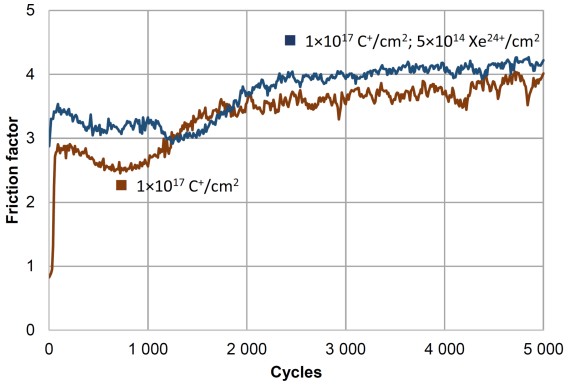

Fig. 11. Coefficient of friction for Ti6Al4V alloy after implantation with carbon ions and additional irradiation with xenon ions.

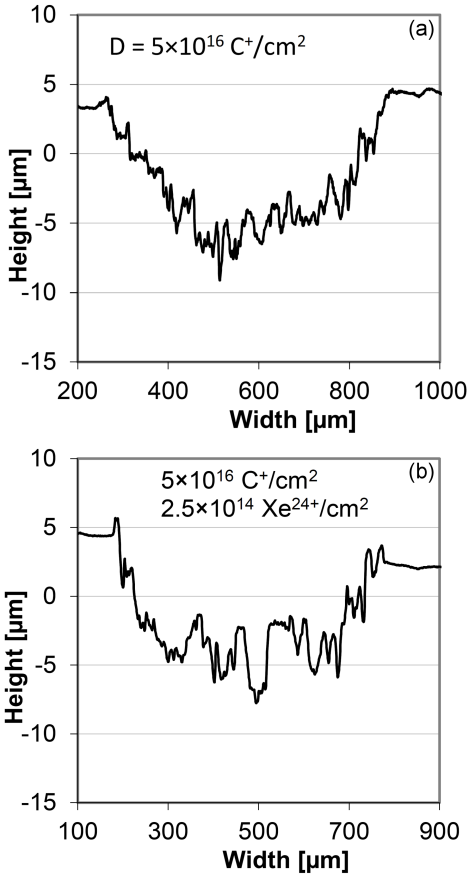

Fig. 12. Profilographs showing the wear track on the Ti6Al4V sample surface after 5000 tribological test cycles: (a) after carbon ion implantation with a fluence of 5×10^{16} C^+/cm^2, (b) after additional irradiation with xenon ions with a fluence of 2.5×10^{14} Xe^{24+}/cm^2.

Figure 12 shows typical profiles of wear track on the surface of the Ti6Al4V alloy after implantation with carbon ions and irradiation with xenon ions. Carbon ion implantation with fluences 1×10^{16} C^+/cm^2 and 5×10^{16} (C^+/cm^2) causes a slight increase in the wear of the implanted sample compared to the unimplanted sample, see Table I. Implantation with fluence 1×10^{17} C^+/cm^2 causes a three-fold decrease in sample wear compared to the unimplanted sample. This sample exhibits the best tribological properties among all tested samples. At the beginning of the tribological test, the coefficient of friction is relatively low, which is due to the formation of a thin DLC layer on the sample surface. Xenon ion irradiation increases the wear of this sample in the tribological test, causes a slight increase in the CoF value and destroys the DLC layer, as can be seen in Fig. 11.

The use of additional irradiation with high-energy xenon ions of the carbon pre-implanted titanium and Ti6Al4V alloy samples leads to their reduced wear. The exception is the Ti6Al4V sample, which was first implanted with a fluence of 1×10^{17} C^+/cm^2 and then irradiated with a fluence of 5×10^{14} Xe^{24+}/cm^2, see Table I.

The distribution of carbon content after irradiating this sample with xenon has a rectangular-like shape. Its wear in tribological tests increased by 3.5 times (Table I). Sample fragments are removed by spalling and abrasive wear with the decreasing oxidative wear (Fig. 13c). After the irradiation facilitating penetration of oxygen into the sample, the role of oxidative wear should be greater than that observed.

The microphotograph of the wear track on the surface of the Ti6Al4V sample before implantation shows the adhesive wear combined with oxidative wear manifested by the smearing of alloy fragments on the track surface (Fig. 13a). Carbon implantation clearly changes the wear characteristics for the Ti6Al4V alloy, which is clearly visible in the SEM photographs (Fig. 12b). A regular smooth track with visible grooves (Fig. 13b) occurs after implantation with a fluence of 1×10^{17} C/cm^2. The distribution of carbon and oxygen content inside the track is similar to the shape of the profilographs. Mechanisms of abrasive and oxidative wear can be observed.

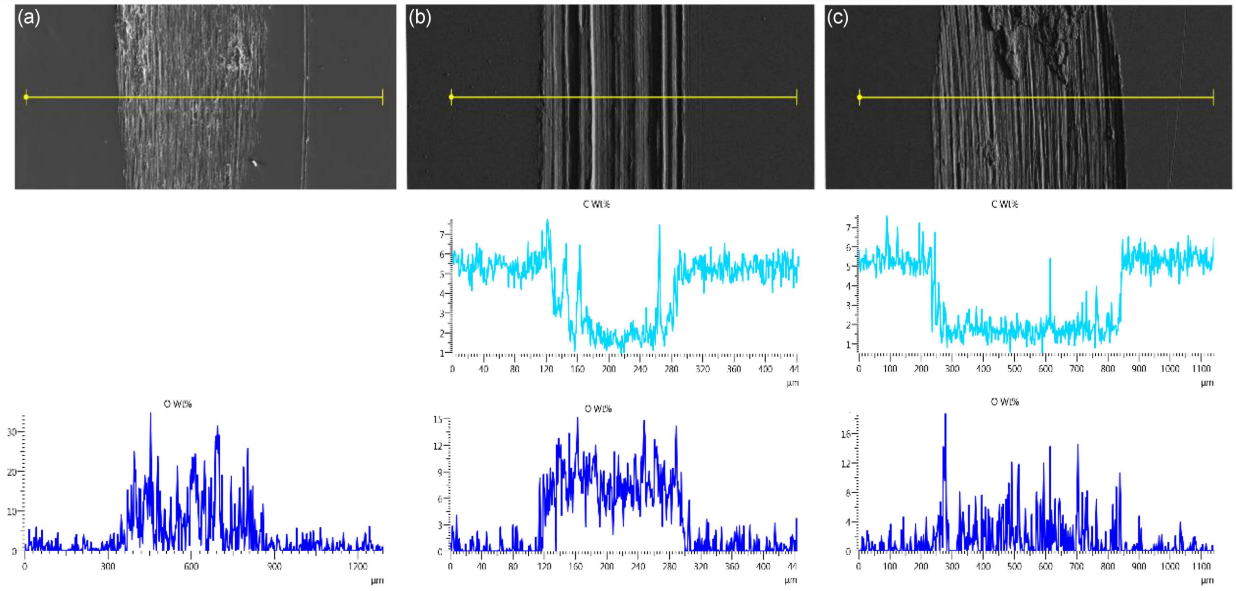

Fig. 13. SEM images of wear track on Ti6Al4V sample: (a) before implantation, (b) after implantation with carbon ions with fluence 1×10^{17} C+/cm^2, (c) after additional irradiation with xenon ions with a fluence of 5×10^{14} Xe^{24+}/cm^2. The carbon and oxygen contents along the scanning line are given below.

3. Discussion

Irradiation significantly changes the topography of the titanium surface, causing local melting of the material. Figure 3c shows grooves with a depth of up to 80 nm, which were produced as a result of the ion beam sweeping across the titanium surface. The melting of the material results from the high energy deposited by the xenon ion beam primarily during the inelastic collision (S_e) with the target electrons.

The CoF variations observed for titanium in the tribological test (Fig. 3) indicate that the surface layer formed during sample preparation (cutting and polishing) plays an important role. The mechanically prepared sample was not annealed in order to maintain conditions similar to those of manufacturing processes. Mechanical processing causes that part of the hcp phase on the titanium surface is transformed into the fcc phase [21]. Defects formed during the sample preparation and the presence of the fcc phase affect the CoF value during the first 1200 test cycles. Chemical interactions and local temperature increase lead to sticking of the sample to the counter sample, as evidenced by large, near-periodic fluctuations in the coefficient of friction observed above 1000 tribological test cycles (Fig. 4). This sticking leads to the smearing of the titanium layers along the track (SEM photograph in Fig. 8a). Although carbon ion implantation slightly increases the coefficient of friction, it eliminates the CoF fluctuations above 1200 tribological test cycles that are characteristic of the unimplanted sample. The CoF fluctuations do not disappear until the end of the tribological test, when the depth of the track is about 10 μm and exceeds the initial range of implanted ions by 25 times.

Carbon ion implantation leads to the formation of hard titanium carbide, which increases CoF of titanium samples and significantly their wear (Table I). The presence of hard TiC causes spalling of small fragments from the sample during tribological tests. Part of the carbon is removed with the wear products. The remaining carbon acts as a lubricant and thus reduces local variations in CoF. Carbon ion implantation also leads to increased wear of the samples. Carbon implantation causes the formation of a thin DLC layer with minimal values of CoF and wear. The DLC layer is formed already during implantation with a fluence of 5×10^{16} C$^+$/cm^2. The thickness of this layer depends on the fluence of carbon ions. Implantation with the maximum fluence 1×10^{17} C$^+$/cm^2 leads to the formation of a thin diamond-like carbon layer on the surface of the sample with a minimal CoF value. The layer is destroyed after irradiation with xenon ions. Following the implantation and irradiation, the titanium samples show the same wear characteristics as the samples that were not subjected to these processes, see Table I. Carbon implantation changes the mechanism of wear for titanium — from dominant adhesive wear to adhesive-abrasive wear. Irradiation, which facilitates the oxygen penetration into the sample, promotes increased oxidative wear.

Carbon ion implantation causes a decrease in the coefficient of friction for the Ti6Al4V alloy (Fig. 10). The decrease of CoF grows with ion fluence. The

fluence of 1×10^{17} C^+/cm^2 causes a 3-fold decrease in the wear of the implanted sample compared to the unimplanted sample (Table I). The wear track is narrow and smooth, see Fig. 13b. The oxidative wear mechanism is dominant. Irradiation of the Ti6Al4V alloy pre-implanted with carbon ions leads to an increase in its coefficient of friction. Irradiation destroys the DLC layer (Fig. 11), which was formed as a result of implantation with a maximum fluence of $D = 1 \times 10^{17}$ C^+/cm^2.

4. Conclusions

The implantation of 120 keV carbon ion increases the coefficients of friction and wear of technically pure titanium. This results from increased adhesive and abrasive wear. The 160 MeV xenon ion irradiation of pre-implanted samples destroys their DLC layer and causes considerable oscillating fluctuations in their coefficients of friction, which is characteristic of unimplanted samples subjected to over 1200 tribological test cycles. The carbon ion implantation of the Ti6Al4V alloy decreases its coefficient of friction. This is the opposite effect to that observed for technically pure titanium. Irradiation of the carbon pre-implanted Ti6Al4V alloy increases its coefficient of friction during the tribological test. Irradiation destroys the DLC layer in both metals. There is no synergistic effect of changes in the tribological properties of titanium and Ti6Al4V alloy resulting from the combined use of the carbon ion implantation and the xenon ion irradiation.

Acknowledgments

The project/research was financed in the framework of the project Lublin University of Technology-Regional Excellence Initiative, funded by the Polish Ministry of Science and Higher Education (contract no. 030/RID/2018/19).

References

[1] A. Amroussia, M. Avilov, C.J. Boehler, F. Durantel, C. Grygiel, W. Mittig, I. Monnet, F. Pellemoin, *Nucl. Instrum. Methods Phys. Res. B* **365**, 515 (2015).

[2] I. Gurrappa, *Mater. Charact.* **51**, 131 (2003).

[3] P. Budzyński, A.A. Youssef, J. Sielanko, *Wear* **261**, 1271 (2006).

[4] P. Budzyński, A.A. Youssef, Z. Surowiec, R. Paluch, *Vacuum* **81**, 1154 (2007).

[5] P. Budzyński, *Nucl. Instrum. Methods Phys. Res. B* **342**, 1 (2015).

[6] P. Budzyński, L .Kara, T. Küçükömeroğlu, M. Kamiński, *Vacuum* **122A**, 230 (2015).

[7] P. Budzyński, J. Sielanko, *Acta Phys. Pol. A* **128**, 841 (2015).

[8] P. Budzyński, M.Kamiński, M. Wiertel, K. Pyszniak, A. Droździel, *Acta Phys. Pol. A* **132**, 203 (2017).

[9] P. Budzyński, M. Kamiński, M. Turek, M. Wiertel, *Wear* **456-457**, 203360 (2020).

[10] J. Sasaki, K. Hayashi, K. Sugiyama, O. Ichiko, Y. Hashiguchi, *Surf. Coat. Technol.* **65**, 160 (1994).

[11] C. Pierret, L. Maunoury, I. Monnet, S. Bouffard, A. Benyagou, I.C. Grygie, D. Busardo, D. Muller, D. Höche, *Wear* **319**, 19 (2014).

[12] R. Rani, N. Kumar, D.D. Kumar, K. Panda, S.K. Srivastava, S. Dash, A.K. Tyagi, *Tribol. Int.* **104**, 121 (2016).

[13] J. Jagielski, L. Thomé, *Vacuum* **81**, 1352 (2007).

[14] J. Jagielski, L. Thomé, *Appl. Phys. A* **97**, 147 (2009).

[15] A. Debelle, S. Moll, B. Decamps, A. Declemy, A. Thome, G. Sattonnay, F. Garrido, I. Jóźwik, J. Jagielski, *Scr. Mater.* **63**, 665 (2010).

[16] P. Budzyński, M. Kamiński, Z. Surowiec, M. Wiertel, V.A. Skuratov, E.A. Korneeva, *Tribol. Int.* **156**, 106854 (2021).

[17] A. Wasy Zia, in: *Advances in Smart Coatings and Thin Films for Futural Industrial and Biomedic Engineering Applications*, Ch. 11, Eds. A.S. Hamdy Makhlouf, N.Y. Abu-Thabit, 2020, p. 307.

[18] Yu.P. Sharkeev, E.V. Kozlov, *Surf. Coat. Technol.* **219**, 158 (2002).

[19] J. Dryzek, P. Horodek, M. Dryzek, *Appl. Phys. A* **124**, 451 (2018).

[20] P. Budzyński, V.A. Skuratov, T. Kochański, *Trib. Inter.* **42**, 1067 (2009).

[21] M. Kamiński, P. Budzyński, Z. Surowiec, M. Wiertel, V.A. Skuratov, *Int. J. Mat. Res.* **109**, 779 (2018).

[22] P. Budzyński, V.A. Skuratov, T. Kochański, Z. Surowiec, *Vacuum* **83**, 190 (2009).

[23] A. Dutta Gupta, P. Mukherjee, N. Gayathri, P. Bhattacharyya, M. Bhattacharya, A. Sarkar, S. Sen, M.K. Mitra, *Nucl. Instrum Methods Phys. Res. B* **387**, 63 (2016).

[24] P. Budzyński, A.A. Youssef, B. Kamieńska, *Vacuum* **70**, 417 (2003).

[25] J.F. Ziegler, M.D. Ziegler, J.P. Biersack, *Nucl. Instrum. Methods Phys. Res. B* **268**, 1818 (2010).

[26] F.C. Salvadom, F. Teixeira-Dias, S.M. Walley, L.J. Lea, J.B. Cardoso, *Prog. Mater. Sci.* **88**, 186 (2017).

[27] P. Budzyñski, M. Kamiński, M. Wiertel, K. Pyszniak, A. Droździel, *Acta Phys. Pol. A* **132**, 203 (2017).

[28] M. Łępicka, M. Grądzka-Dahlke, I. Zaborowska, G. Górski, R. Mosdorf, *Tribol. Int.* **165**, 107342 (2022).

[29] M. Łępicka, G. Gorski, M. Grądzka-Dahlke, R. Mosdorf, *Tribol. Int.* **151**, 106402 (2020).